volume (BV/TV), trabecular number (Tb.N) and trabecular spaces (Tb.Sp) in nasal and frontal bones were quantified by μCT. Data presented were means± s.d. by three different skulls and three independent experiments. *$p<0.05$, **$p<0.005$.

Fig. 6. A mechanism by which enhanced BMP signaling develops craniosynostosis in mice. In wild–type skull, BMPR1A (green) exerts both Smad-dependent and -independent signaling upon ligand binding (left panel). In the mutant mice (*ca-Bmpr1a:P0-Cre*) which has a constitutively active form of BMPR1A (purple), basal levels of Smad-dependent signaling are upregulated and it is further increased upon ligand binding. Increases of phospho-ERK1/2 are also observed due to the increase of FGF signaling (middle panel). In the rescued mice (*ca-Bmpr1a:P0-Cre:Bmpr1a*$^{+/-}$), removal of one copy of endogenous BMPR1A normalizes levels of Smad-dependent signaling leading to the phenotypic rescue of premature suture fusions and skull morphology (right panel). Enhanced levels of FGF-ERK signaling are still observed in the rescued mice but it may be not sufficient to induce morphological malformations, i.e., FGF signaling in *ca-Bmpr1a:P0-Cre:Bmpr1a*$^{+/-}$ mice does not attain levels needed to develop craniosynostosis (see discussion),.

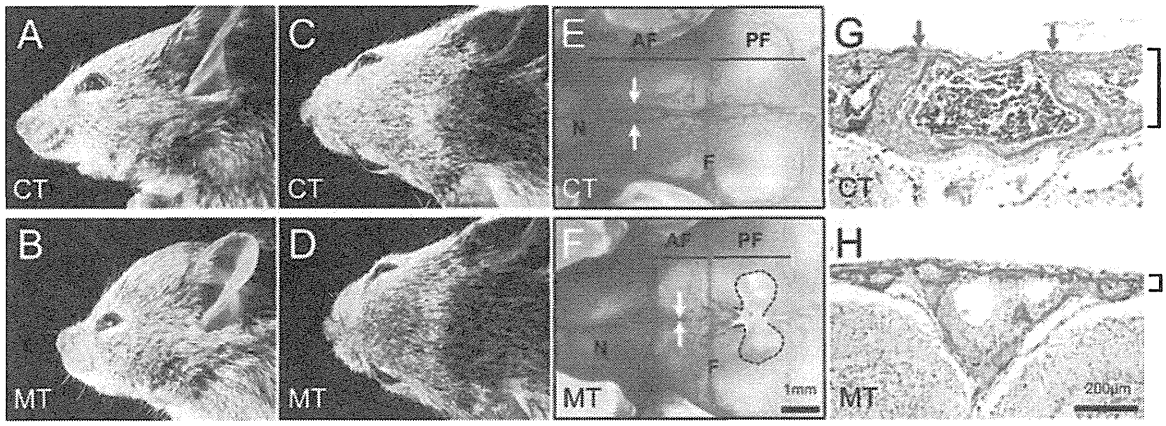

Figure 1

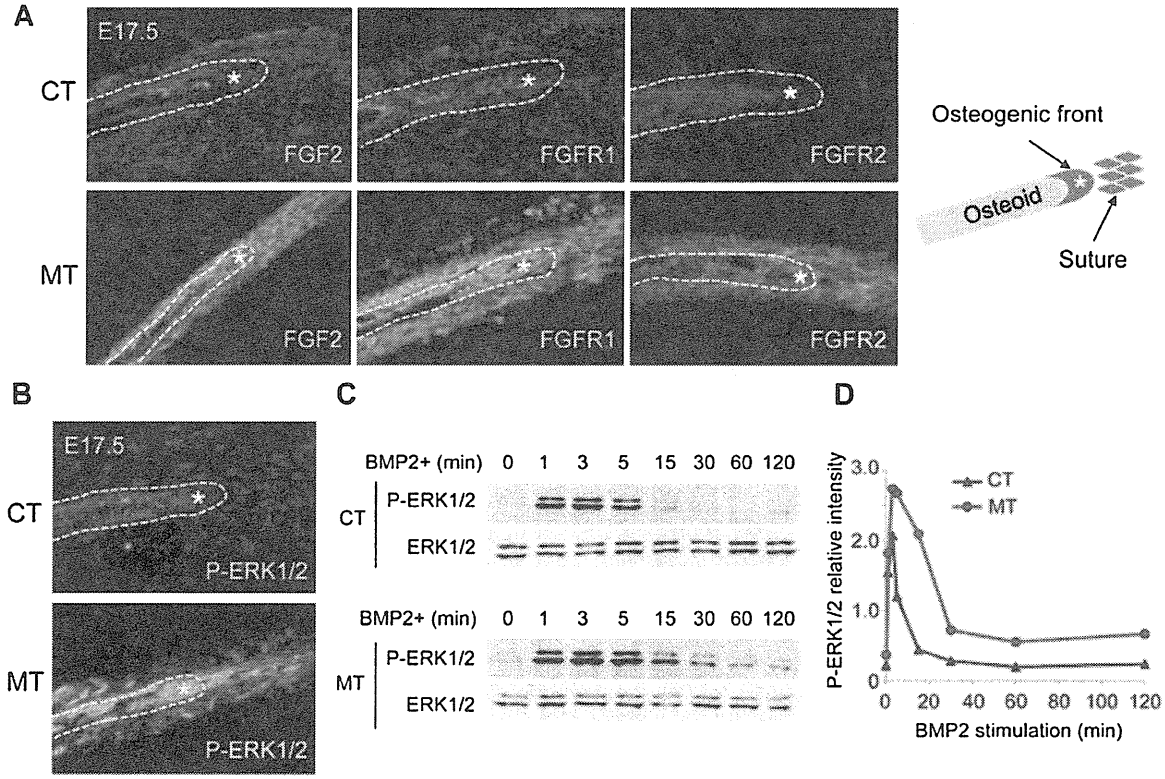

Figure 2

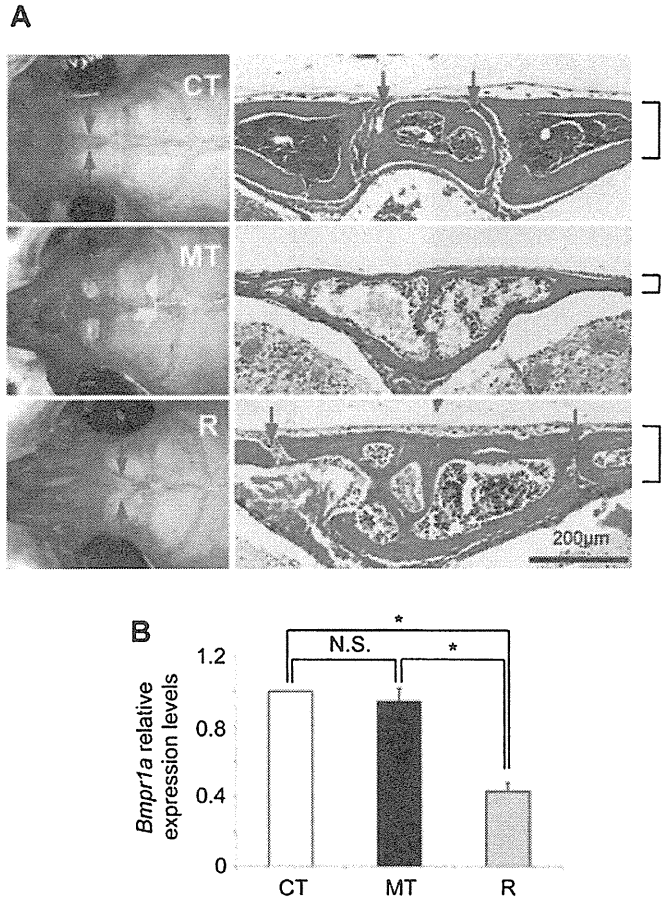

Figure 3

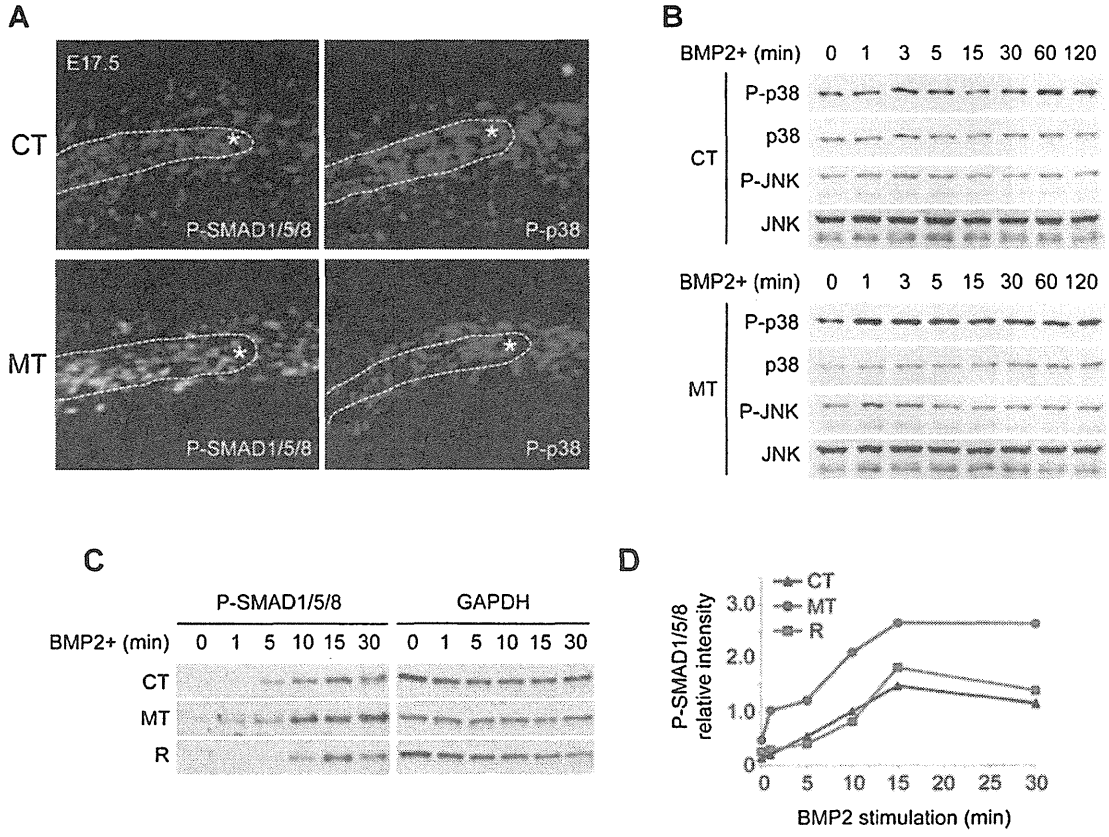

Figure 4

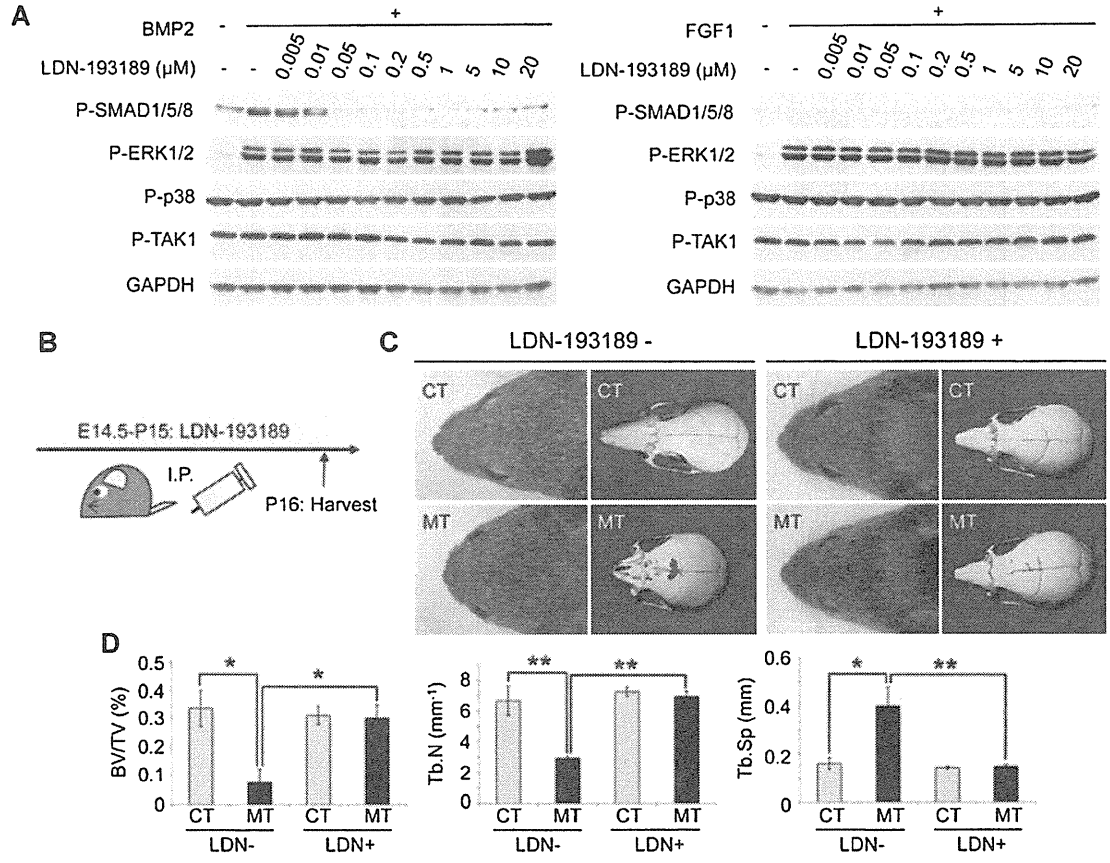

Figure 5

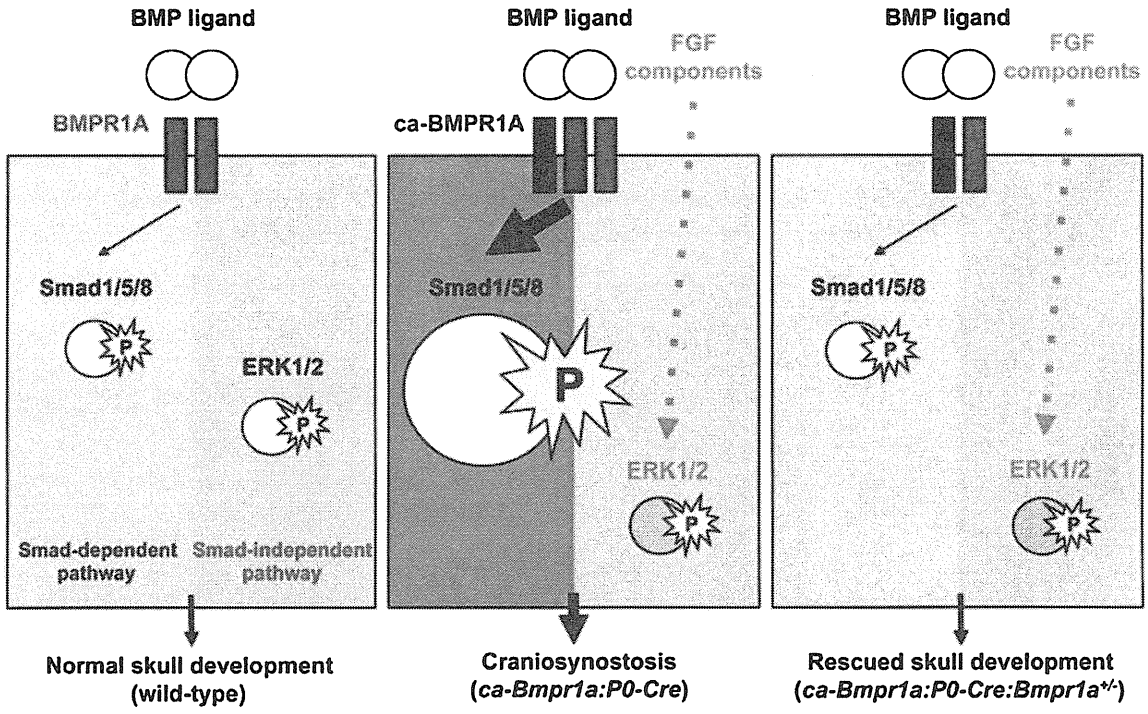

Figure 6

Mol. Cells 33, 259-267, March 31, 2012
DOI/10.1007/s10059-012-2227-z

Molecules and Cells

CD99-Dependent Expansion of Myeloid-Derived Suppressor Cells and Attenuation of Graft-Versus-Host Disease

Hyo Jin Park[1,7], Dahye Byun[2,7], An Hi Lee[3,7], Ju Hyun Kim[1], Young Larn Ban[4], Masatake Araki[5], Kimi Araki[5], Ken-ichi Yamamura[5], Inho Kim[6], Seong Hoe Park[1,4], and Kyeong Cheon Jung[1,4,*]

CD99 is involved in many cellular events, such as the generation of Hodgkin and Reed-Sternberg cells, T cell co-stimulation, and leukocyte transendothelial migration. However, these studies have been limited to *in vitro* or *in vivo* experiments using CD99-deficient cell lines or anti-CD99 antibodies. In the present study, using CD99-deficient mice established by the exchangeable gene trap method, we investigated the physiologic function of murine CD99. In a B6 splenocytes → bm12 graft-versus-host disease model, wild-type cells were minimally lethal, whereas all mice that received CD99-deficient donor cells developed an early and more severe pathology. Graft-versus-host disease in these mice was associated with insufficient expansion of myeloid-derived suppressor cells. This was confirmed by experiments illustrating that the injection of wild-type donor cells depleted of Mac-1$^+$ cells led to an almost identical disease course as the CD99-deficient donor system. Therefore, these results suggest that CD99 plays a crucial role in the attenuation of graft-versus-host disease by regulating the expansion of myeloid-derived suppressor cells.

INTRODUCTION

Human CD99, encoded by the *MIC2* gene in pseudoautosomal region 1 (PAR1) of the X chromosome, is a ubiquitous 32 kDa transmembrane protein with a highly O-glycosylated extracellular region (Hahn et al., 1997; Park et al., 2005). It is expressed in all leukocyte lineages and involved in many cellular events. Engagement of CD99 on human thymocytes with agonistic antibodies induces homotypic aggregation (Hahn et al., 1997), apoptosis (Bernard et al., 1997), and upregulation of TCR and MHC class molecules on the surface of thymocytes (Choi et al., 1998). In mature T cells, CD99 delivers effective co-stimulatory signals (Oh et al., 2007). In B cells, the downregulation of CD99 by EBV-encoded latent membrane protein-1 (LMP-1) leads to the generation of Hodgkin and Reed-Sternberg cells related to Hodgkin's disease (Kim et al., 1998; 2000; Lee et al., 2011). Moreover, transendothelial migration of monocytes is also regulated by human CD99 (Schenkel et al., 2002). In addition to these observations in humans, a mouse homologue of human CD99 (also designated D4) was identified as a ligand of the paired Ig-like type 2 receptor (PILR) (Park et al., 2005; Shiratori et al., 2004). Its functional analogy with human CD99 is supported by reports that it also participates in the transendothelial migration of leukocytes and recruitment into inflamed tissue (Bixel et al., 2004; Dufour et al., 2008). Until recently, however, these studies have been limited to *in vitro* or *in vivo* experiments using CD99-deficient cell lines or anti-CD99 antibody due to the unavailability of CD99-deficient mice.

Myeloid-derived suppressor cells (MDSCs) are a heterogeneous population of activated immature myeloid cells with morphology similar to granulocytes or monocytes (Movahedi et al., 2008) that accumulate under numerous pathologic conditions including cancer, infection, inflammatory disease, and stress (Gabrilovich and Nagaraj, 2009). MDSCs are characterized by the co-expression of myeloid-cell lineage differentiation antigen Gr-1 and CD11b (Mac-1) in mice (Gabrilovich and Nagaraj, 2009). MDSC expansion and activation are influenced by several factors, representative of which are cyclooxygenase 2 (also known as PTGS2) and vascular endothelial growth factor (VEGF), which are produced by tumor cells, tumor stromal cells, and activated T cells (Gabrilovich and Nagaraj, 2009). These factors are mainly involved in the upregulation of immune suppressive factors in MDSCs and their expansion. MDSCs were recently reported to play a potentially important role in determining the severity of graft-versus-host disease (GVHD) (Rao et al., 2003) by suppressing alloreactivity (Highfill et al., 2010; Morecki et al., 2008).

In the present study, we found that there was significant aggravation of GVHD when splenocytes of CD99-deficient mice

[1]Department of Pathology, Seoul National University College of Medicine, Seoul 110-799, Korea, [2]Department of Biomedical Science, Seoul National University College of Medicine, Seoul 110-799, Korea, [3]Department of Pathology, The Catholic University Incheon St. Mary's Hospital, Incheon 403-016, Korea, [4]Graduate School of Immunology, Seoul National University College of Medicine, Seoul 110-799, Korea, [5]Institute of Resource Development and Analysis, Kumamoto University, Kumamoto, 860-0811, Japan, [6]Department of Internal Medicine, Seoul National University College of Medicine, Seoul 110-799, Korea, [7]These authors contributed equally to this work.
*Correspondence: jungkc66@snu.ac.kr

Received October 17, 2011; revised December 30, 2011; accepted January 11, 2012; published online February 15, 2012

Keywords: CD99, graft versus host disease, myeloid cells

were used as donor cells. In subsequent experiments to identify the mechanism by which CD99 is related to the disease course of GVHD, we found that expansion of MDSCs is severely compromised in the absence of CD99.

MATERIALS AND METHODS

Mice

A heterozygote mutant C56BL/6 mouse clone ($CD99^{+/GT}$) with an insertional mutation between exons 2 and 3 of the CD99 gene (21-B6T44 clone in Exchangeable Gene Trap Clone database; http://egtc.jp/action/access/clone_detail?id=21-B6T44) was produced using the pU-21T exchangeable gene trap vector and deposited in the Center for Animal Resources and Development (CARD) R-BASE of the Kumamoto University of Japan (http://cardb.cc.kumamoto-u.ac.jp/transgenic/index.jsp). Wild-type C57BL/6J (B6, H-2^b), B6.C-H2bm12/KhEg (bm12), and CD45.1 congenic B6 mice were purchased from the Jackson Laboratory (USA). $CD99^{GT/GT}$ mice were backcrossed to $CD45.1^+$ congenic B6 mice to generate $CD45.1^+$ $CD99^{GT/GT}$ mice. All mice were maintained at the Center for Animal Resource and Development at Seoul National University. The animal studies were performed after receiving approval from the Institutional Animal Care and Use Committee (IACUC) of Seoul National University (IACUC approval No. SNU-091125-5).

Genotyping of $CD99^{GT/GT}$ mice

DNA samples for $CD99^{GT/GT}$ genotyping were extracted from the tails of mice and PCR was performed using tail genomic DNA as a template. For wild-type alleles, a 5′ primer (5′-CGA GTGACGACTTCAACCTGGGC-3′) located in exon 2 and a 3′ primer (5′-TGAGTCTCCGTGTGGCCTTG-3′) located in exon 5 were used to generate a 917 bp wild-type fragment. PCR was performed for 35 cycles (60 s at 94°C; 60 s at 60°C; 60 s at 72°C). To detect the trap allele, a 5′Z-1 primer (5′-GCGTTACC CAACTTAATCG-3′) and a 3′ Z-2 primer (5′-TGTGAGCGAGT AACAACCCG-3′) located in the pU21 were used to generate a 320 bp fragment. For amplification of the 3′ flanking region of the trap vector, a 5′ primer (5′-AAGGCCCCAACGCCCAAGA AGCC-3′) located in exon 3 and a 3′ primer (5′-AGGGCGTCC TCCAGG TCGAA-3′) located in exon 4 were used.

Reverse transcriptase-polymerase chain reaction (RT-PCR) analysis

Total cellular RNA was prepared from spleens using the RNeasy Mini kit (Qiagen, USA) according to the manufacturer's instructions. cDNA was synthesized using oligo-dT primers, and used as a template for PCR with the following primers: mouse CD99, 5′ primer (5′-CCAGTGACGACTTCAACCTG-3′) and 3′ primer (5′-GATAGGCCACGAAGCTCGACAC-3′); mouse β-actin, 5′ primer (5′-GACGGCCAGGTCATCACTAT-3′) and 3′ primer (5′-GTACTTGCGCTCAGGAGGAG-3′).

Antibodies and flow cytometric analysis

FITC-, PE-, and APC-anti-mouse CD4 (RM4.5), CD8 (53-6.7), PE-anti-mouse CD11b (M1/70), APC-anti-mouse CD11c (HL3), PerCy5.5-anti-mouse CD45.1 (A20), FITC-anti-mouse B220 (RA3-6B2), APC-anti-mouse NK1.1 (PK136), FITC-anti-mouse TCRβ (H57-597), APC-anti-mouse Gr-1 (RB6-8C5) antibodies, and APC-streptavidin were purchased from eBioscience (USA) or BD Biosciences (USA). PE- and biotin-conjugated anti-mouse CD99 (EJ2) monoclonal antibody was obtained from Dinona (Korea). Fresh cell suspensions of thymocytes, splenocytes, and lymph nodes were stained with antibodies and then analyzed using a flow cytometer (FACSCalibur; BD, USA) and CellQuest Pro software (BD, USA).

Induction of GVHD

Recipient bm12 mice received 600 cGy of irradiation from a ^{137}Cs source split into two doses and separated by 4 h. One day later, 1.5×10^7 unfractionated spleen cells from B6 mice were intravenously injected into irradiated recipients. For adoptive transfer of fractionated cells, splenocytes were subjected to magnetic cell sorting (Miltenyi Biotec, USA), according to the manufacturer's instructions, and purity was usually greater than 95%. To compare the development of GVHD between recipients of fractionated and unfractionated populations, the number of $CD4^+$ T cells injected into each mouse was equalized. At the indicated times, the bone marrow and spleen cells were harvested for flow cytometric analysis, and the cytokine concentration in serum was measured by cytometric bead array (BD).

Suppressor assay

To investigate the *in vitro* suppressor activity of MDSCs, a mixed lymphocyte reaction was performed. $CD4^+$ T cells were purified from CD45.1 B6 mice via magnetic sorting and labeled with CFSE as described previously (Lo et al., 2011). CD45.1 B6-derived Mac-1^+Gr-1^+ MDSCs were purified from the spleens of bm12 mice, who had received CD45.1 B6 splenocytes, via flow cytometric sorting. T cell-depleted splenocytes were purified from B6 mice via magnetic sorting. CFSE-labeled $CD4^+$ T cells (3×10^5) and 2,000 rad-irradiated bm12 splenocytes (3×10^5) were cultured in the presence of either sorted MDSCs or T cell-depleted B6 splenocytes (3×10^5). After 5 days' culture, cells were stained with anti-CD4 and anti-CD45.1 antibodies and the percentage of $CFSE^{lo}$ cells in the gated $CD45.1^+CD4^+$ population was measured via flow cytometric analysis.

EL4 tumor model

Mice were subcutaneously injected with 5×10^6 EL4 cells and monitored every 2 to 3 days to evaluate tumor growth. Subcutaneous tumors were measured with calipers along the perpendicular axis of the tumor and size was expressed as tumor volume based on the following formula: tumor volume (mm^3) = (major axis) × (minor axis)^2 × 0.52 (Li et al., 2004).

Statistical analysis

All data were analyzed using GraphPad Prism software (GraphPad Software, USA). Time curves for progression to death were prepared by the Kaplan-Meier method. Significance between animal groups was computed using a *t*-test. A value of $p < 0.05$ was considered statistically significant.

RESULTS

Systemic deletion of CD99 does not affect the cellularity of spleen leukocyte subpopulations

To investigate the physiological role of mouse CD99 in the development and function of immune cells, heterozygote 21-B6T44 clone mice, in which pU-21T exchangeable gene trap vectors were inserted into the CD99 (pilr-l) gene, were intercrossed, and the offspring were screened via PCR analysis of genomic DNA. When primer sets specific for the inserted gene trap vector or targeted to exon 2 and exon 5 of the mouse CD99 gene were used, insertion of the gene trap vector between exons 2 and 3 of the CD99 gene caused the wild-type allele to be unamplified and thus the genotype was easily identified (Fig. 1A, upper and middle). We also excluded the possibility that a large deletion in the 3′ flanking region of the trap

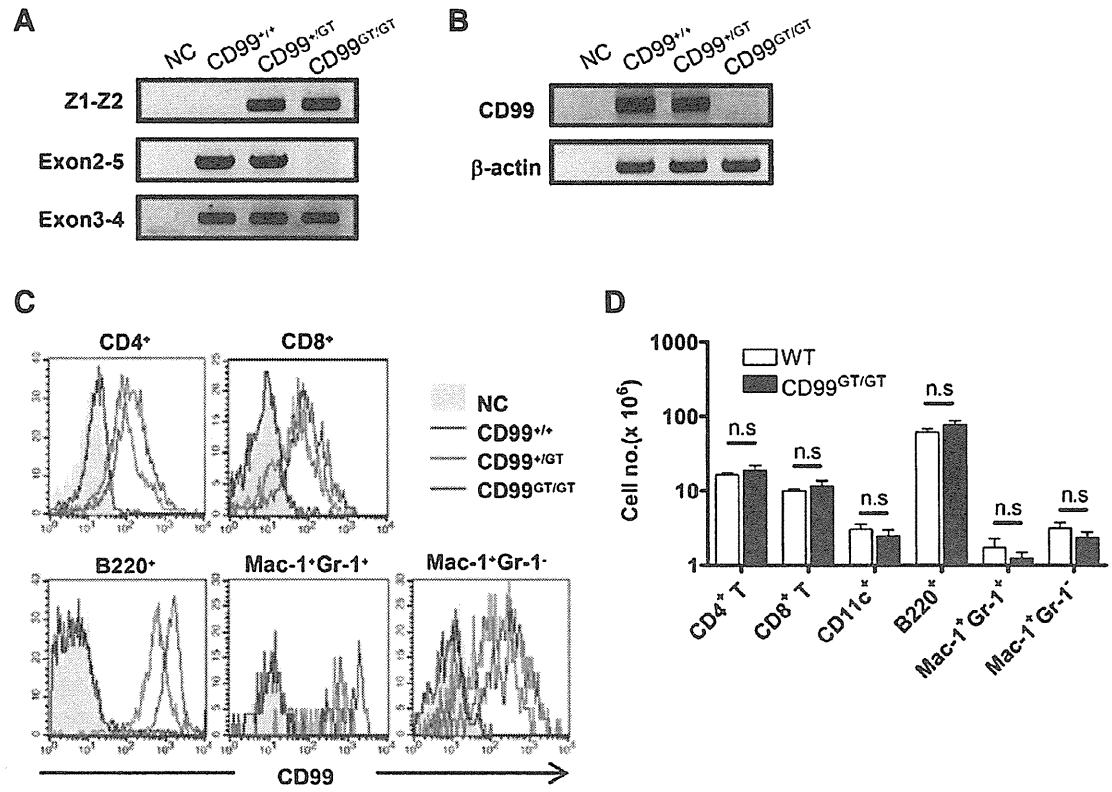

Fig. 1. Genotypic and phenotypic analysis of wild-type mice and insertional mutants in CD99 via gene trap. (A) Representative results of PCR genotyping. To detect wild-type and trap alleles, genomic DNA was prepared from the tails of wild-type ($CD99^{+/+}$), heterozygous ($CD99^{+/GT}$), and homozygous insertional mutant ($CD99^{GT/GT}$) mice, amplified using a primer pair that detected the pU-21T gene trap vector, murine CD99 exons 2 and 5, or murine CD99 exons 3 and 4, and analyzed in parallel with a negative control (NC). (B) Absence of CD99 gene transcripts in $CD99^{GT/GT}$ splenocytes. RT-PCR analysis of splenocytes obtained from wild-type, $CD99^{+/GT}$, and $CD99^{GT/GT}$ mice demonstrated the expression of CD99 transcripts only in wild-type and $CD99^{+/GT}$ mice. Transcription of β-actin was used as a positive control. (C) No expression of CD99 protein on the surface of $CD99^{GT/GT}$ splenocytes. Flow cytometric analysis of splenocytes gated on each population revealed higher CD99 expression on the surface of B cells ($B220^+$) and $Mac\text{-}1^+Gr\text{-}1^+$ cells than that of T cells and macrophages ($Mac\text{-}1^+Gr\text{-}1^-$). CD99 expression level in $CD99^{+/GT}$ mice was about two-fold lower than that of wild-type littermates. (D) Cellularity of each leukocyte subpopulation in spleen is not affected by CD99 deletion. The absolute number of splenic cell subsets of wild-type and $CD99^{GT/GT}$ mice was calculated based on the relative proportion determined by flow cytometry. The data represent five mice per group. n.s, not significant.

vector was present, via amplification of the region encompassing the exons 3 and 4 of the CD99 gene (Fig. 1A, lower). The absence of CD99 gene transcripts in the homozygote mutant was confirmed via RT-PCR analysis of RNA extracted from the spleen (Fig. 1B), whereas the expression of CD99 in wild-type spleens has been documented (Park et al., 2005).

Next, we compared CD99 expression in spleen cell subpopulations using flow cytometry (Fig. 1C). Consistent with our RT-PCR results, CD99 was not expressed in splenocytes of homozygous mutant mice. In wild-type B6 mice, the expression level of CD99 in B cells and $Mac\text{-}1^+Gr\text{-}1^+$ cells was higher than that in T cells. In the splenocytes of heterozygous mice ($CD99^{+/GT}$), the CD99 expression level was half of that of the wild-type. Systemic deletion of CD99 did not affect the cellularity of each leukocyte subpopulation in spleen (Fig. 1D) and both heterozygote and homozygote mice appeared normal and were fertile.

Development of lethal GVHD and insufficient expansion of MDSCs in irradiated bm12 mice that received $CD99^{GT/GT}$ splenocytes

To compare the immune function of CD99-deficient mice to that of wild-type mice, we used a GVHD model, which was generated by B6 splenocyte transfer into irradiated MHC class II-different bm12 hosts (B6 splenocytes → bm12) (Rao et al., 2003). In accordance with previous descriptions (Rao et al., 2003; Sprent et al., 1990; 1995), when unfractionated splenocytes from B6 mice were transferred into sublethally irradiated bm12 mice, host mice recovered their body weight after transient weight loss during the first week post-transplant and showed minimal lethality during the 10-week follow-up period (Fig. 2A). In contrast, inoculation with CD99-deficient splenocytes caused continuous weight loss in recipients resulting in early death of all $CD99^{GT/GT}$ splenocytes → bm12 mice (Fig. 2A). In agreement with the clinical course of the disease, CD99 deficiency in donor cells caused a more severe drop in cellularity of host cells in spleen and bone marrow (Fig. 2B, left).

In the B6 splenocytes → bm12 GVHD model, the donor non-T cell compartment represses $CD4^+$ T cell-mediated acute GVHD (Rao et al., 2003). The clinical course in bm12 mice transplanted with purified B6 $CD4^+$ T cells in that study was similar to that of bm12 mice that received $CD99^{GT/GT}$ splenocytes in the present study. Based on these findings, we assessed

whether the lack of CD99 expression in donor splenocytes affected the non-T cell compartment. Seven days after donor cell transfer, there was no statistically significant difference in the number of donor cells in spleens of bm12 mice that received wild-type and CD99-deficient splenocytes (Fig. 2B, right, and Table 1). During the next 7 days, there was a three-fold increase in the total number of donor cells in the spleens of wild-type cell recipients (Fig. 2B, right, and Table 1). Specifically, a marked increase in the number of Mac-1$^+$Gr-1$^+$ MDSCs (about 22-fold) contributed to the major change in donor cell number, and thus donor cells were composed of 40% MDSCs, which were more abundant than CD4$^+$ T cells 14 days after transplant (Table 1 and Fig. 2C). This was in sharp contrast to the three-fold increase in the number of CD99-deficient MDSCs during the same period (Table 1). In contrast, there was less difference in the cell numbers of other donor-derived cell populations between the two groups of mice (Table 1). Therefore, taken together, these results suggest that CD99 may modulate GVHD progression by promoting the expansion of MDSCs.

Table 1. Summary of donor cell numbers in recipient spleens

Donor cell type	Days	Cell no. (mean ± SE × 10^5)*			Fold change	
		CD99$^{+/+}$	CD99$^{GT/GT}$	p	CD99$^{+/+}$	CD99$^{GT/GT}$
Total	7	59 ± 10	49 ± 11	0.53	3.4	1.6
	14	197 ± 30	76 ± 11	0.002		
CD4$^+$ T	7	31 ± 5	23 ± 5	0.32	1.2	0.9
	14	36 ± 7	20 ± 3	0.06		
CD8$^+$ T	7	12 ± 2	10 ± 2	0.43	2.0	1.4
	14	25 ± 6	14 ± 2	0.07		
B cell	7	8 ± 2	5 ± 1	0.15	1.5	1.0
	14	13 ± 4	5 ± 1	0.04		
Mac-1$^+$Gr-1$^+$	7	4 ± 1	6 ± 1	0.22	21.6	2.7
	14	84 ± 13	16 ± 5	0.0005		

*Number of mice in each group: CD99$^{+/+}$ day 7 (n = 4), CD99$^{GT/GT}$ day 7 (n = 5), CD99$^{+/+}$ day 14 (n = 4), CD99$^{GT/GT}$ day 14 (n = 6).

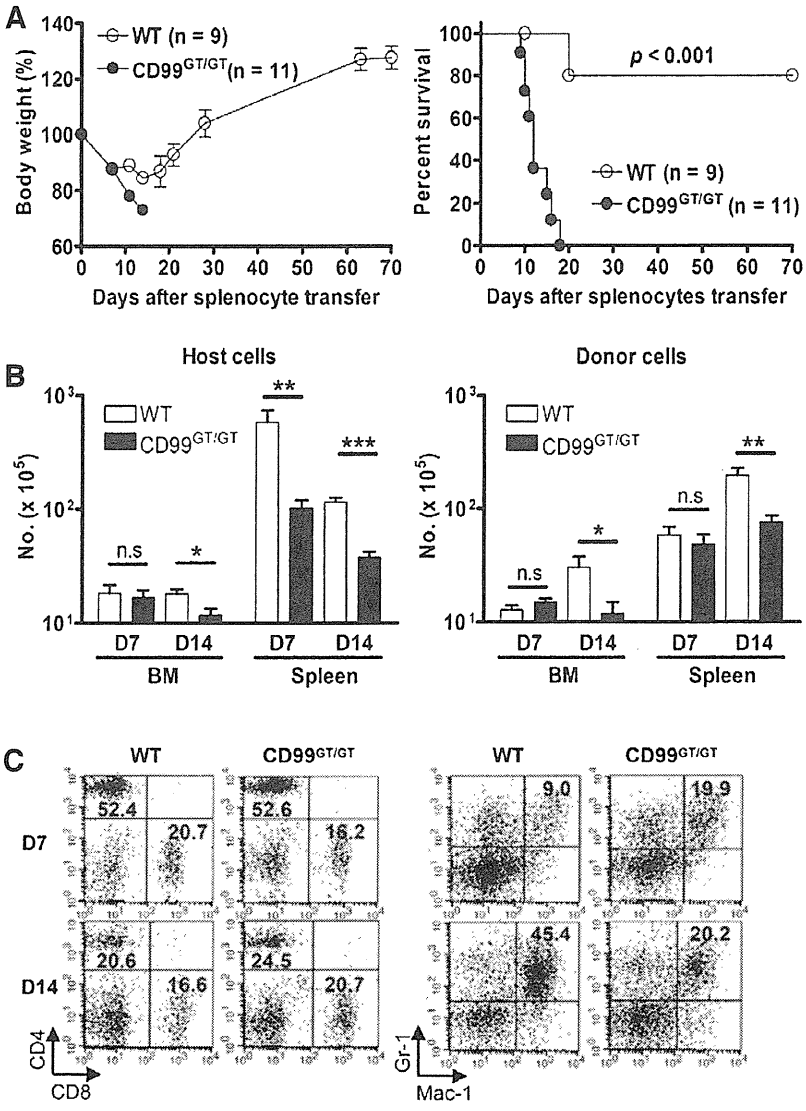

Fig. 2. The absence of CD99 on donor cells aggravates acute GVHD in MHC class II-only disparate recipients. (A) Early death of bm12 mice that received CD99$^{GT/GT}$ splenocytes compared to recipients of wild-type cells. Sublethally irradiated bm12 mice were infused with 1.5 × 10^7 splenocytes obtained from wild-type (WT) or CD99$^{GT/GT}$ donor mice on day 0. Mice were monitored for body weight (left) and survival (right). Data are pooled from two independent experiments and numbers in parentheses are the total number of recipient mice in each group. (B) Decreased expansion of CD99-deficient donor cells, compared to wild-type cells in bm12 mice. To assess the severity of GVHD, cells in bone marrow (BM) and spleen were analyzed by flow cytometry on days 7 and 14 after adoptive transfer, and the absolute number of host (left) and donor (right) cells were calculated by multiplying the percentage of CD45.1$^-$ (host) and CD45.1$^+$ (donor) by the cellularity. Data are mean values ± SEM from four to six animals in each group and representative data from two independent experiments are shown. (C) Defect in the expansion of donor-derived Mac-1$^+$Gr-1$^+$ MDSCs in bm12 mice that received CD99$^{GT/GT}$ splenocytes compared to recipients of wild-type cells. To evaluate the fraction of donor CD4$^+$ T cells, CD8$^+$ T cells, and Mac-1$^+$Gr-1$^+$ MDSCs, cells from the spleens of recipient bm12 mice were stained with the indicated antibodies on days 7 and 14 after adoptive transfer of 1.5 × 10^7 wild-type or CD99-deficient splenocytes and were analyzed by flow cytometry. Representative data from three independent experiments are shown. n.s, not significant; *, P < 0.05; **, P < 0.01, ***, P < 0.001.

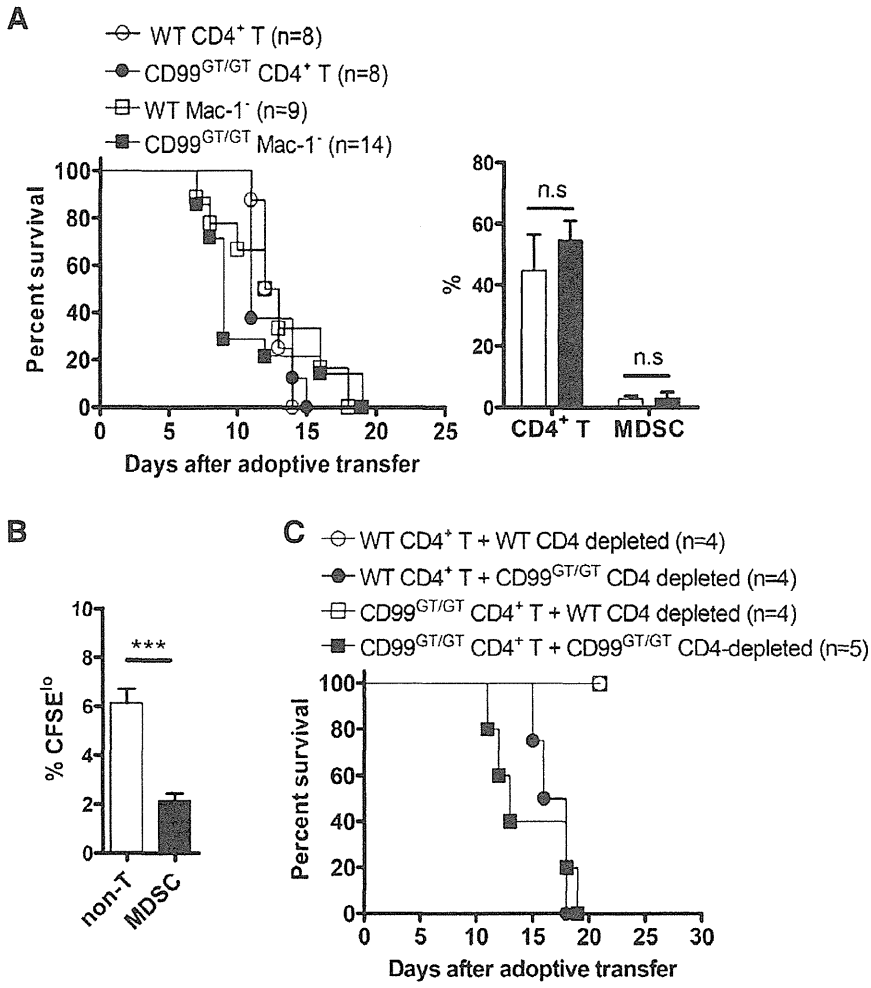

Fig. 3. Essential role of CD99 in the non-lymphoid population for suppression of GVHD. (A) Accelerated mortality of bm12 mice received Mac-1-depleted splenocytes from wild-type or CD99$^{GT/GT}$ mice. Groups of bm12 mice received purified CD4$^+$ T cells (2.5×10^6) or Mac-1-depleted cells (Mac-1$^-$; 1.5×10^7) from wild-type (WT) or CD99$^{GT/GT}$ mice on day 0. The survival rate pooled from two independent experiments is shown, and numbers in parentheses indicate the total number of recipient mice in each group (left). The percentages of CD4$^+$ T cells and Mac-1$^+$Gr-1$^+$ MDSCs among the donor cells in the spleens of recipients were also measured via flow cytometric analysis on day 10 after adoptive transfer, and data are mean values ± SEM from three animals in each group (right). (B) MDSCs suppress T cell alloresponse *in vitro*. CFSE-labeled CD45.1 B6 CD4$^+$ T cells were stimulated with irradiated bm12 splenocytes in the presence of either T cell-depleted B6 splenocytes (non-T) or Mac-1$^+$Gr-1$^+$ MDSCs derived from donor cells in bm12 mice received B6 splenocytes. After 5 days' culture, the percentage of CFSE^{lo} cells in the gated CD4$^+$ T population was compared via flow cytometric analysis. (C) The suppression of GVHD progress depends on the CD99 in the non-T cell population. Purified CD4$^+$ T cells (2.5×10^5) were co-transferred with CD4-depleted cells (1.25×10^7) into sublethally irradiated bm12 mice as indicated; survival rate is shown. Numbers in parentheses are the total number of recipient mice in each group.

Defect in MDSC expansion from CD99-deficient donor cells accelerates lethal GVHD

To determine whether the defect in MDSC expansion culminates in the accelerated mortality of CD99$^{GT/GT}$ splenocytes → bm12 mice, we transferred purified CD4$^+$ T cells or Mac-1-depleted splenocytes from B6 mice into the sublethally irradiated bm12 mice. Consistent with a previous report (Rao et al., 2003), injection of CD4$^+$ T cells caused rapid disease and the survival rate was not affected by the lack of CD99 in donor cells (Fig. 3A, left), indicating that CD99 expressed on CD4$^+$ T cells had no influence on their alloreactivity. Moreover, groups of mice that received Mac-1-depleted splenocytes from wild-type or CD99$^{GT/GT}$ mice also followed a similar disease course (Fig. 3A, left). In the spleens of these recipients, the fraction of donor-derived MDSCs was markedly reduced by Mac-1-depletion prior to adoptive transfer (Fig. 3A, right). To further investigate whether MDSCs could suppress the alloreactivity of CD4$^+$ T cells, donor-derived Mac-1$^+$Gr-1$^+$ MDSCs, which expanded after transfer of wild-type splenocytes to irradiated bm12 mice, were purified, and CFSE-labeled CD45.1 B6 CD4$^+$ T cells were stimulated with irradiated bm12 splenocytes in the presence of MDSCs or T cell-depleted B6 splenocytes as a negative control. After 5 days' culture, about 6% of CD4$^+$ T cells in control wells showed diluted CFSE (Fig. 3B). In contrast, MDSCs inhibited the proliferation of CD4$^+$ T cells. Thus, these data support the suggestion that the compromised expansion of donor-derived MDSCs might cause acute lethal GVHD in recipients of CD99-deficient splenocytes.

In the B6 splenocytes → bm12 GVHD model, a difference at a single MHC class II allele between donor and recipient leads the donor CD4$^+$ T cells to act as the main alloreactive cells (Rao et al., 2003; Sprent et al., 1990). Consequently, to investigate whether CD99 in CD4$^+$ T cells or other cell populations are relevant for sufficient MDSC expansion, CD4-depleted splenocytes were infused into irradiated bm12 mice along with CD4$^+$ T cells. Notably, wild-type CD4-negative fraction co-transferred with wild-type or CD99-deficient CD4$^+$ T cells protected the recipient mice from acute GVHD (Fig. 3C). In contrast, the absence of CD99 in the CD4-negative donor cell fraction did not ameliorate the symptoms of acute GVHD, independent of CD99 expression by the donor CD4$^+$ T cells. Therefore, these data suggest that MDSC expansion in the B6 splenocytes → bm12 model depends on CD99 molecules in the donor cell population other than alloreactive T cells.

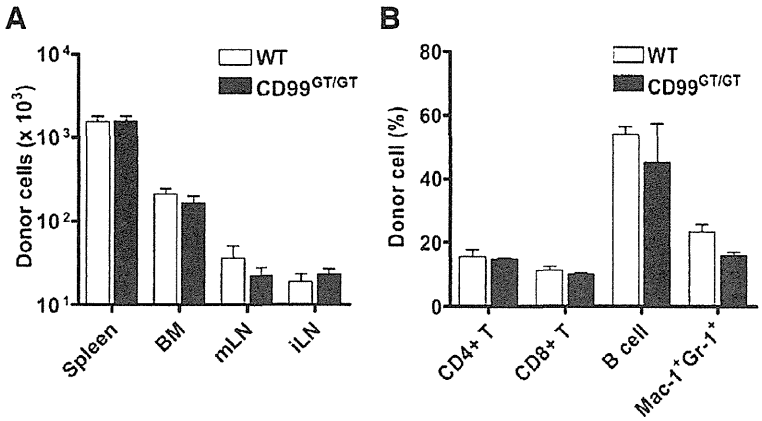

Fig. 4. Comparable migration properties of wild-type and CD99-deficient MDSCs. (A) The absolute number of CD99$^{GT/GT}$ and wild-type donor cells in the spleen, bone marrow, and lymph nodes of recipient mice was similar. Splenocytes (1.5×10^7) from CD45.1$^+$ wild-type (WT) or CD99$^{GT/GT}$ mice were injected into sublethally irradiated bm12 mice, and 24 h after cell transfer the number of donor cells was calculated by multiplying the percentage of CD45.1$^+$ cells by the total cell number in the spleen, bone marrow (BM), mesenteric lymph node (mLN), and inguinal lymph node (iLN). (B) Comparable homing activities of T cells, B cells, or MDSCs between CD99$^{GT/GT}$ and wild-type donors. Cells in the spleen were stained with antibodies against CD45.1, CD4, CD8, B220, Mac-1, and Gr-1, and the donor cell fraction in each subset was analyzed by flow cytometry. The data are mean values ± SEM from four recipients in each group and representative data from two independent experiments are shown.

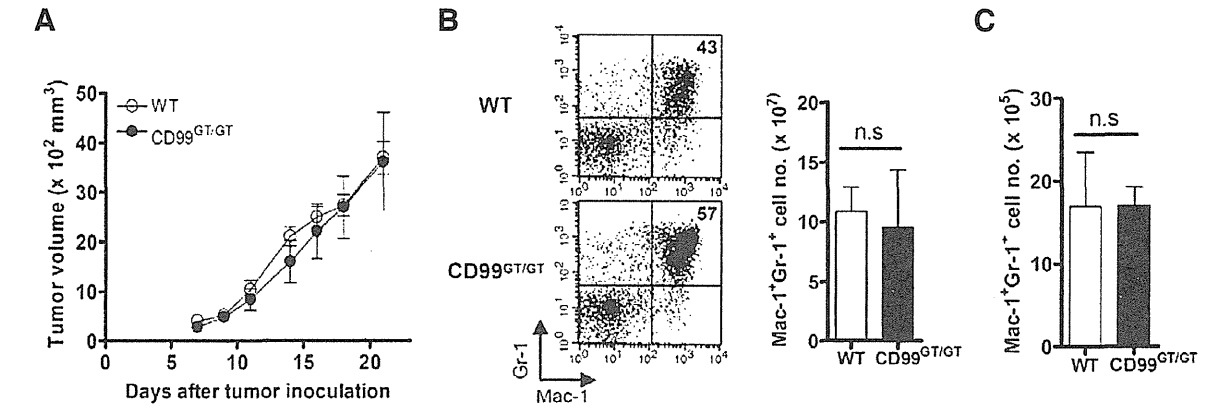

Fig. 5. CD99-independent expansion of MDSCs in tumor-bearing mice. (A) Similar tumor growth rate in CD99$^{GT/GT}$ and wild-type mice. Wild-type (WT) and CD99$^{GT/GT}$ mice were injected subcutaneously with 5×10^6 EL4 cells. Tumor growth was measured using calipers and average tumor volume was obtained from the width and length of the tumor. (B, C) MDSC expansion in tumor-bearing mice is independent on the CD99 expression status of host mice. The Mac-1$^+$Gr-1$^+$ MDSC fraction in the spleen (B) and tumor (C) of EL-4 tumor-bearing wild-type and CD99$^{GT/GT}$ mice was assessed by flow cytometry. A respresentative flow cytometric prolife is presented (B, left), and the total number of MDSCs in the spleen (B, right) and tumor (C) in wild-type ($n = 4$) or CD99-deficient ($n = 3$) mice 3 weeks after tumor challenge was calculated. Representative data from three independent experiments are shown. n.s, not significant.

Comparable migration properties of CD99-deficient and wild-type MDSCs

Murine CD99 participates in transendothelial migration of T cells, neutrophils, and monocytes (Bixel et al., 2004; 2007; Dufour et al., 2008). Therefore, we tested the possibility that accelerated GVHD in CD99$^{GT/GT}$ splenocytes → bm12 mice is secondary to altered migratory properties of CD99$^{GT/GT}$ splenocytes compared to wild-type cells. Splenocytes from CD45.1$^+$ congenic wild-type or CD99$^{GT/GT}$ mice were injected into sublethally irradiated bm12 hosts. Twenty-four hours later, the absolute number of CD45.1$^+$ CD99$^{GT/GT}$ and wild-type cells in the spleen, bone marrow, and lymph nodes of the recipient mice were similar (Fig. 4A). Further analysis of donor cell subpopulations in the spleen showed no significant difference in homing activities of T cells, B cells, or MDSCs between CD99$^{GT/GT}$ and wild-type donors (Fig. 4B), suggesting that the difference in the migratory properties of the donor cells was unlikely to account for the contrasting GVHD phenotypes induced by CD99$^{GT/GT}$ and wild-type donors.

CD99-independent expansion of MDSCs in tumor-bearing mice

MDSCs accumulate in cancer patients and animal models (Gabrilovich and Nagaraj, 2009). To evaluate the role of CD99 in the cancer-induced expansion of MDSCs, mice were subcutaneously injected with 5×10^6 EL4 cells and tumor growth was monitored every 2 or 3 days. There was no difference between wild-type and CD99$^{GT/GT}$ mice (Fig. 5A). After 3 weeks, tumor-bearing mice were sacrificed to measure MDSCs in the spleen and tumor by flow cytometry. In both types of mice, Mac-1$^+$Gr-1$^+$ MDSCs markedly expanded (Fig. 5B left) and their number in the spleens or tumors of both groups did not differ (Fig. 5B right, and Fig. 5C). Thus, tumor-induced expansion of MDSCs does not depend on CD99 molecules.

Comparable serum soluble factor concentrations between CD99-deficient and wild-type groups

The expansion and activation of MDSCs is influenced by several factors, such as IL-1β, IL-4, IL-6, IL-10, IL-13, GM-CFS, and IFN-γ (Gabrilovich and Nagaraj, 2009). Some of these

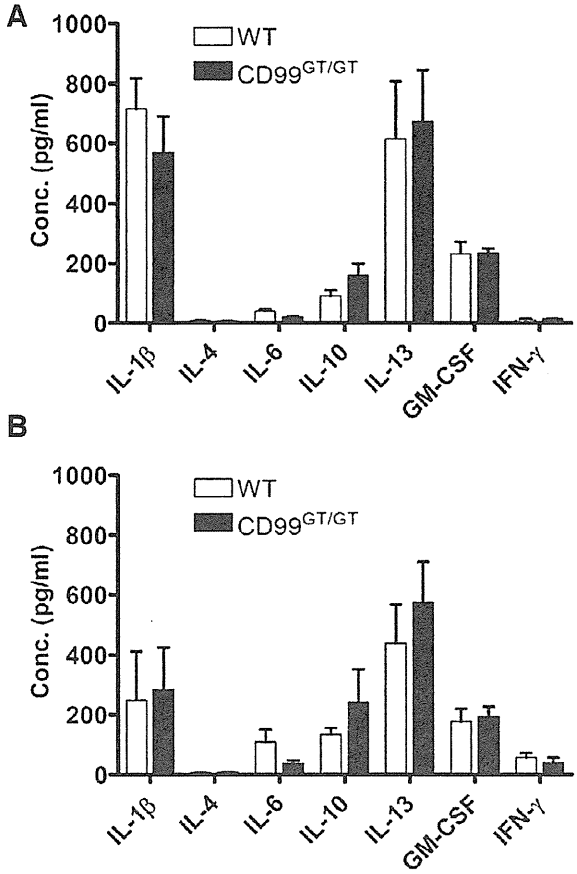

Fig. 6. Comparable serum concentration of soluble factors that induce the expansion and activation of MDSCs between CD99-deficient and wild-type groups. (A) No difference in serum IL-1β, IL-4, IL-6, IL-10, IL-13, GM-CFS, and IFN-γ concentrations between bm12 mice that received wild-type (WT) and CD99-deficient ($CD99^{GT/GT}$) splenocytes. Serum cytokine levels were analyzed by cytometric bead array on day 7 after adoptive transfer. Data are mean values ± SEM from five animals in each group. (B) No difference in serum cytokine concentration between tumor-bearing wild-type and CD99-deficient ($CD99^{GT/GT}$) mice. Data are mean values ± SEM from five animals in each group 3 weeks after tumor challenge.

cytokines are produced primarily by tumor cells and others are produced by activated T cells and tumor stromal cells. This raises the possibility that CD99 expression in donor cells might affect the serum concentration of these soluble factors and thereby modulate the expansion of MDSCs in the GVHD model. To test this possibility, sera were collected from bm12 mice on day 7 after adoptive transfer of wild-type or CD99-deficient splenocytes, and serum cytokine concentrations were compared. As shown in Fig. 6A, there was no difference in serum IL-1β, IL-4, IL-6, IL-10, IL-13, GM-CFS, and IFN-γ concentrations between the two groups. This was also the case in the tumor-bearing mouse model (Fig. 6B).

DISCUSSION

In the present work, we investigated the physiologic function of CD99 using CD99-deficient mice. Systemic deletion of CD99 by the exchangeable gene trap method did not affect the cellularity of leukocyte subpopulations in the spleen. Unlike wild-type donor cells, however, CD99-deficient splenocytes caused lethal GVHD when adoptively transferred into irradiated bm12 hosts. In this GVHD model, we found that expansion of donor-derived MDSCs and the resulting attenuation of acute GVHD were dependent on CD99. On the contrary, tumor-induced expansion of MDSCs in CD99-deficient mice was comparable to that of wild-type mice.

To investigate the physiologic function of CD99, we used a CD99 mutant mouse clone established by the exchangeable gene trap method (EGTC 21-B6T44). The trap vector was confirmed to be inserted between exons 2 and 3 of the CD99 gene in the 21-B6T44 mouse clone via 5′ RACE. The absence of a CD99 transcript and protein expression in the homozygous mutants of this clone was confirmed by RT-PCR and flow cytometry. Then we investigated the *in vivo* impact of CD99 deficiency using a well-defined GVHD model in mutant MHC class II-different mice (Rao et al., 2003; Sprent et al., 1990). The most remarkable finding in bm12 mice that received CD99-deficient splenocytes was that they succumbed to lethal acute GVHD. The early lethality in these recipients was in sharp contrast to the clinical course in recipients of wild-type B6 splenocytes where there was minimal lethality (Sprent et al., 1990; 1995). This type of acute GVHD also developed in bm12 mice that received either purified B6 $CD4^+$ T cells alone or B6 $ccr2^{-/-}$ total splenocytes (Rao et al., 2003). Previous results obtained from $ccr2^{-/-}$ mice led to the hypothesis that cross-talk between the T cell and non-T cell compartments is important for amelioration of acute GVHD and that this interaction is dysregulated in B6 $ccr2^{-/-}$ splenocytes → bm12 mice (Rao et al., 2003). Here, we analyzed the Mac-1^+Gr-1^+ population in recipient mice during the course of GVHD, as MDSCs increase in numerous pathologic conditions and have suppressive effects on the adaptive immune response (Gabrilovich and Nagaraj, 2009). As expected, the donor MDSC population increased markedly during the second week post-transplantation in B6 splenocytes → bm12 mice but not in recipients of CD99-deficient splenocytes. Moreover, depletion of the Mac-1^+ fraction from donor cells prior to transplantation caused identical disease course regardless of CD99 expression in donor cells. Therefore, these findings suggest that MDSCs might be the major player responsible for repression of alloreactive $CD4^+$ T cells, and that MDSC expansion requires CD99 expression in donor cells.

While CD99 operated in the expansion of MDSCs in GVHD, this was not the case in the tumor model. The expansion and activation of MDSCs in a tumor system requires several soluble factors, which are spontaneously produced from tumor or stromal cells rather than as a result of cross-talk via cell-cell interaction (Gabrilovich and Nagaraj, 2009). These factors include prostaglandins (Sinha et al., 2007), VEGF (Gabrilovich et al., 1998), stem cell factor (SCF) (Pan et al., 2008), GM-CSF (Serafini et al., 2004), M-CSF (Menetrier-Caux et al., 1998), and inflammatory cytokines such as IL-6 and IL-1β (Bunt et al., 2007; Song et al., 2005). In contrast, during the development of GVHD, suppression of this pathology seems to primarily need diverse cross-talk between immune cells. In particular, in the B6 splenocytes → bm12 GVHD model, the development of GVHD is dominantly dependent on the $CD4^+$ T cells, as the only haplotype difference in donor and recipient mice is located on a single MHC class allele, $I\text{-}A^b$. Thus, under these circumstances, it seems that the interaction between alloreactive T cells and non-T cell compartments might contribute to the expansion of MDSCs in a CD99-dependent manner.

We next addressed whether cell migration was impaired by the lack of CD99 molecules, given that CD99 may play an im-

portant role in the *in vitro* transendothelial migration of human monocytes (Schenkel et al., 2002), and *in vivo* blocking studies using anti-CD99 antibodies support the idea that murine CD99 plays a significant role in the migration of T cells, neutrophils, and monocytes to a site of inflammation (Bixel et al., 2004; 2007; Dufour et al., 2008). However, we found contradictory results; there was no difference in migratory activities between wild-type and CD99-deficient leukocytes. Although the reason for this apparent discrepancy is not clear, two possibilities may be considered. In our system, cell migration was designed to be directed to the lymphoid organs, whereas in other model systems, cells were directed to the inflammatory foci. In addition, other researchers used blocking antibodies for simple physical inhibition of CD99 molecules. In contrast, our model was a $CD99^{GT/GT}$ mouse system where cells can modulate other redundant molecules involved in transmigration, such as PECAM-1, ICAM-2, junctional adhesion molecules (JAMs), and endothelial cell-selective adhesion molecule (ESAM) (Vaporciyan et al., 1993; Vestweber, 2007; Woodfin et al., 2010).

In summary, we found that massive expansion of donor MDSCs after leukocyte transplantation ameliorates acute GVHD and that CD99 plays a major role in the efficient expansion of these cells. Considering that the only known ligand of murine CD99 is PILR, which is expressed on the surface of leukocytes (Shiratori et al., 2004), ligation of CD99 in MDSCs by PILR in $CD4^+$ T cells is a candidate cellular mechanism for promotion of MDSC expansion. Conversely, ligation of PILR in $CD4^+$ T cells by CD99 in MDSCs or other non-T cells might affect T cell function, such as the secretion of cytokines that regulate MDSC expansion. In the present study, no difference in serum cytokine concentration was found between bm12 mice that received CD99-deficient and wild-type splenocytes, supporting the former possibility. However, it remains to be clarified whether direct contact between effector T cells and non-T cell compartments through PILR-CD99 interaction is involved in MDSC expansion.

ACKNOWLEDGMENTS

This work was supported by the National Research Foundation (NRF) through the Tumor Immunity Medical Research Center at Seoul National University College of Medicine, Korea (R13-2002-025-01003-0). The English in this document has been checked by at least two professional editors of an English editing company, "Textcheck".

REFERENCES

Bernard, G., Breittmayer, J.P., de Matteis, M., Trampont, P., Hofman, P., Senik, A., and Bernard, A. (1997). Apoptosis of immature thymocytes mediated by E2/CD99. J. Immunol. *158*, 2543-2550.

Bixel, G., Kloep, S., Butz, S., Petri, B., Engelhardt, B., and Vestweber, D. (2004). Mouse CD99 participates in T-cell recruitment into inflamed skin. Blood *104*, 3205-3213.

Bixel, M.G., Petri, B., Khandoga, A.G., Khandoga, A., Wolburg-Buchholz, K., Wolburg, H., Marz, S., Krombach, F., and Vestweber, D. (2007). A CD99-related antigen on endothelial cells mediates neutrophil but not lymphocyte extravasation *in vivo*. Blood *109*, 5327-5336.

Bunt, S.K., Yang, L., Sinha, P., Clements, V.K., Leips, J., and Ostrand-Rosenberg, S. (2007). Reduced inflammation in the tumor microenvironment delays the accumulation of myeloid-derived suppressor cells and limits tumor progression. Cancer Res. *67*, 10019-10026.

Choi, E.Y., Park, W.S., Jung, K.C., Kim, S.H., Kim, Y.Y., Lee, W.J., and Park, S.H. (1998). Engagement of CD99 induces upregulation of TCR and MHC class I and II molecules on the surface of human thymocytes. J. Immunol. *161*, 749-754.

Dufour, E.M., Deroche, A., Bae, Y., and Muller, W.A. (2008). CD99 is essential for leukocyte diapedesis *in vivo*. Cell Commun. Adhes. *15*, 351-363.

Gabrilovich, D.I., and Nagaraj, S. (2009). Myeloid-derived suppressor cells as regulators of the immune system. Nat. Rev. Immunol. *9*, 162-174.

Gabrilovich, D., Ishida, T., Oyama, T., Ran, S., Kravtsov, V., Nadaf, S., and Carbone, D.P. (1998). Vascular endothelial growth factor inhibits the development of dendritic cells and dramatically affects the differentiation of multiple hematopoietic lineages *in vivo*. Blood *92*, 4150-4166.

Hahn, J.H., Kim, M.K., Choi, E.Y., Kim, S.H., Sohn, H.W., Ham, D.I., Chung, D.H., Kim, T.J., Lee, W.J., Park, C.K., et al. (1997). CD99 (MIC2) regulates the LFA-1/ICAM-1-mediated adhesion of lymphocytes, and its gene encodes both positive and negative regulators of cellular adhesion. J. Immunol. *159*, 2250-2258.

Highfill, S.L., Rodriguez, P.C., Zhou, Q., Goetz, C.A., Koehn, B.H., Veenstra, R., Taylor, P.A., Panoskaltsis-Mortari, A., Serody, J.S., Munn, D.H., et al. (2010). Bone marrow myeloid-derived suppressor cells (MDSCs) inhibit graft-versus-host disease (GVHD) via an arginase-1-dependent mechanism that is up-regulated by interleukin-13. Blood *116*, 5738-5747.

Kim, S.H., Choi, E.Y., Shin, Y.K., Kim, T.J., Chung, D.H., Chang, S.I., Kim, N.K., and Park, S.H. (1998). Generation of cells with Hodgkin's and Reed-Sternberg phenotype through downregulation of CD99 (Mic2). Blood *92*, 4287-4295.

Kim, S.H., Shin, Y.K., Lee, I.S., Bae, Y.M., Sohn, H.W., Suh, Y.H., Ree, H.J., Rowe, M., and Park, S.H. (2000). Viral latent membrane protein 1 (LMP-1)-induced CD99 down-regulation in B cells leads to the generation of cells with Hodgkin's and Reed-Sternberg phenotype. Blood *95*, 294-300.

Lee, E.K., Chae, J.H., and Kang, M.S. (2011). Nuclear factor-κB2 represses Sp1-mediated transcription at the CD99 promoter. Mol. Cells *32*, 555-560.

Li, Q., Pan, P.Y., Gu, P., Xu, D., and Chen, S.H. (2004). Role of immature myeloid Gr-1+ cells in the development of antitumor immunity. Cancer Res. *64*, 1130-1139.

Lo, D.J., Weaver, T.A., Stempora, L., Mehta, A.K., Ford, M.L., Larsen, C.P., and Kirk, A.D. (2011). Selective targeting of human alloresponsive CD8+ effector memory T cells based on CD2 expression. Am. J. Transplant *11*, 22-33.

Menetrier-Caux, C., Montmain, G., Dieu, M.C., Bain, C., Favrot, M.C., Caux, C., and Blay, J.Y. (1998). Inhibition of the differentiation of dendritic cells from CD34(+) progenitors by tumor cells: role of interleukin-6 and macrophage colony-stimulating factor. Blood *92*, 4778-4791.

Morecki, S., Gelfand, Y., Yacovlev, E., Eizik, O., Shabat, Y., and Slavin, S. (2008). CpG-induced myeloid CD11b+Gr-1+ cells efficiently suppress T cell-mediated immunoreactivity and graft-versus-host disease in a murine model of allogeneic cell therapy. Biol. Blood Marrow Transplant *14*, 973-984.

Movahedi, K., Guilliams, M., Van den Bossche, J., Van den Bergh, R., Gysemans, C., Beschin, A., De Baetselier, P., and Van Ginderachter, J.A. (2008). Identification of discrete tumor-induced myeloid-derived suppressor cell subpopulations with distinct T cell-suppressive activity. Blood *111*, 4233-4244.

Oh, K.I., Kim, B.K., Ban, Y.L., Choi, E.Y., Jung, K.C., Lee, I.S., and Park, S.H. (2007). CD99 activates T cells via a costimulatory function that promotes raft association of TCR complex and tyrosine phosphorylation of TCR zeta. Exp. Mol. Med. *39*, 176-184.

Pan, P.Y., Wang, G.X., Yin, B., Ozao, J., Ku, T., Divino, C.M., and Chen, S.H. (2008). Reversion of immune tolerance in advanced malignancy: modulation of myeloid-derived suppressor cell development by blockade of stem-cell factor function. Blood *111*, 219-228.

Park, S.H., Shin, Y.K., Suh, Y.H., Park, W.S., Ban, Y.L., Choi, H.S., Park, H.J., and Jung, K.C. (2005). Rapid divergency of rodent CD99 orthologs: implications for the evolution of the pseudoautosomal region. Gene *353*, 177-188.

Rao, A.R., Quinones, M.P., Garavito, E., Kalkonde, Y., Jimenez, F., Gibbons, C., Perez, J., Melby, P., Kuziel, W., Reddick, R.L., et al. (2003). CC chemokine receptor 2 expression in donor cells serves an essential role in graft-versus-host-disease. J. Immunol. *171*, 4875-4885.

Schenkel, A.R., Mamdouh, Z., Chen, X., Liebman, R.M., and Muller, W.A. (2002). CD99 plays a major role in the migration of monocytes through endothelial junctions. Nat. Immunol. *3*, 143-150.

Serafini, P., Carbley, R., Noonan, K.A., Tan, G., Bronte, V., and

Borrello, I. (2004). High-dose granulocyte-macrophage colony-stimulating factor-producing vaccines impair the immune response through the recruitment of myeloid suppressor cells. Cancer Res. *64*, 6337-6343.

Shiratori, I., Ogasawara, K., Saito, T., Lanier, L.L., and Arase, H. (2004). Activation of natural killer cells and dendritic cells upon recognition of a novel CD99-like ligand by paired immunoglobulin-like type 2 receptor. J. Exp. Med. *199*, 525-533.

Sinha, P., Clements, V.K., Fulton, A.M., and Ostrand-Rosenberg, S. (2007). Prostaglandin E2 promotes tumor progression by inducing myeloid-derived suppressor cells. Cancer Res. *67*, 4507-4513.

Song, X., Krelin, Y., Dvorkin, T., Bjorkdahl, O., Segal, S., Dinarello, C.A., Voronov, E., and Apte, R.N. (2005). CD11b+/Gr-1+ immature myeloid cells mediate suppression of T cells in mice bearing tumors of IL-1beta-secreting cells. J. Immunol. *175*, 8200-8208.

Sprent, J., Schaefer, M., and Korngold, R. (1990). Role of T cell subsets in lethal graft-versus-host disease (GVHD) directed to class I versus class II H-2 differences. II. Protective effects of L3T4+ cells in anti-class II GVHD. J. Immunol. *144*, 2946-2954.

Sprent, J., Hurd, M., Schaefer, M., and Heath, W. (1995). Split tolerance in spleen chimeras. J. Immunol. *154*, 1198-1206.

Vaporciyan, A.A., DeLisser, H.M., Yan, H.C., Mendiguren, II, Thom, S.R., Jones, M.L., Ward, P.A., and Albelda, S.M. (1993). Involvement of platelet-endothelial cell adhesion molecule-1 in neutrophil recruitment *in vivo*. Science *262*, 1580-1582.

Vestweber, D. (2007). Adhesion and signaling molecules controlling the transmigration of leukocytes through endothelium. Immunol. Rev. *218*, 178-196.

Woodfin, A., Voisin, M.B., and Nourshargh, S. (2010). Recent developments and complexities in neutrophil transmigration. Curr. Opin. Hematol. *17*, 9-17.

 Related Commentary, page 1970

mTORC1 is essential for leukemia propagation but not stem cell self-renewal

Takayuki Hoshii,[1] Yuko Tadokoro,[1] Kazuhito Naka,[1] Takako Ooshio,[1] Teruyuki Muraguchi,[1] Naoyuki Sugiyama,[2] Tomoyoshi Soga,[2] Kimi Araki,[3] Ken-ichi Yamamura,[3] and Atsushi Hirao[1]

[1]Division of Molecular Genetics, Cancer and Stem Cell Research Program, Cancer Research Institute, Kanazawa University, Kanazawa, Japan. [2]Institute for Advanced Biosciences, Keio University, Tsuruoka, Japan. [3]Division of Developmental Genetics, Center for Animal Resources and Development, Institute of Resource Development and Analysis, Kumamoto University, Kumamoto, Japan.

Although dysregulation of mTOR complex 1 (mTORC1) promotes leukemogenesis, how mTORC1 affects established leukemia is unclear. We investigated the role of mTORC1 in mouse hematopoiesis using a mouse model of conditional deletion of *Raptor*, an essential component of mTORC1. *Raptor* deficiency impaired granulocyte and B cell development but did not alter survival or proliferation of hematopoietic progenitor cells. In a mouse model of acute myeloid leukemia (AML), *Raptor* deficiency significantly suppressed leukemia progression by causing apoptosis of differentiated, but not undifferentiated, leukemia cells. mTORC1 did not control cell cycle or cell growth in undifferentiated AML cells in vivo. Transplantation of *Raptor*-deficient undifferentiated AML cells in a limiting dilution revealed that mTORC1 is essential for leukemia initiation. Strikingly, a subset of AML cells with undifferentiated phenotypes survived long-term in the absence of mTORC1 activity. We further demonstrated that the reactivation of mTORC1 in those cells restored their leukemia-initiating capacity. Thus, AML cells lacking mTORC1 activity can self-renew as AML stem cells. Our findings provide mechanistic insight into how residual tumor cells circumvent anticancer therapies and drive tumor recurrence.

Introduction

mTOR is an evolutionarily conserved kinase in eukaryotes that plays a critical role in sensing and responding to factors such as nutrient availability, energy sufficiency, stress, hormones, and mitogens. mTOR forms two complexes, designated mTOR complex 1 (mTORC1) and mTORC2. mTORC1, which consists of mTOR, Raptor, and mLST8, phosphorylates multiple substrates, including p70 ribosomal protein S6 kinase (p70S6K) and eukaryote translation initiation factor 4E binding protein 1 (4E-BP1). These target molecules control cell growth (size) and proliferation by modifying protein translation (1). In addition, mTORC1 regulates mitochondrial biogenesis (2, 3) and autophagy (4). mTORC2, formed by mTOR, Rictor, mLST8, SIN1, and Protor, phosphorylates distinct targets including AKT, RAC1, PKCα, and SGK1 (1, 5). Disruption of mTOR and Raptor in mice promotes early embryonic lethality around the implantation stage, whereas deficiency of Rictor, mLST8, or SIN1 causes embryonic lethality at mid-gestation (6, 7). Thus, mTORC1 is indispensable for cell proliferation and survival in early embryogenesis. Although mTORC1 has been assumed to function in growth and metabolism of most cell types, previous studies of mice lacking *Raptor* only in adipocytes or muscle suggest that mTORC1 may have distinct functions in homeostasis depending on the tissue (8, 9). Specifically, *Raptor* deficiency alters mitochondrial biogenesis differently in adipocytes than in muscle. Thus, it is unclear how mTORC1 contributes to the control of growth, proliferation, survival, and differentiation under physiological conditions.

mTORC1 dysregulation promotes leukemogenesis and depletes HSCs (10–14). The tuberous sclerosis complex (TSC) proteins TSC1 and TSC2 negatively regulate mTORC1 signaling. Following phosphorylation by AKT, TSC2 is destabilized, and repression of mTOR signaling is relieved. *Tsc1* deletion in mice causes defects in cell cycling and HSC function due to enhanced mTORC1 activity (10, 11). Deficiency in *Pten*, a negative regulator of PI3K/AKT signaling, also impairs the quiescence of HSCs, leading to their depletion. *Pten* deficiency in hematopoietic cells promotes myeloproliferative disease followed by development of leukemia (12, 14, 15). Since these phenotypes are inhibited by the mTORC1 inhibitor rapamycin, mTORC1 activation has been thought to induce HSC depletion and leukemogenesis. Currently, however, it is unclear how altered mTORC1 affects the behavior of established leukemia.

Recent improvements in cell purification and transplantation techniques have enabled identification of tumor cells capable of initiating and propagating malignancy, known as cancer stem cells (CSCs). Previous studies have suggested that common mechanisms regulate stem cell properties (stemness) in both HSCs and leukemia stem cells (CSCs in leukemia), leading to the idea that leukemia stem cells may originate from HSCs (16). On the other hand, it has been reported that introduction of oncogene fusion constructs that promote acute myeloid leukemia (AML), such as the *MLL-ENL*, *MLL-AF9*, and *MOZ-TIF2* genes, into committed myeloid progenitors transforms the cells and promotes the acquisition of self-renewal ability (17–21). A recent study using a large number of primary human AML patient samples indicated that human AML stem cells are immunophenotypically similar to progenitors, including lymphoid-primed multipotential progenitors and granulocyte-macrophage progenitors (GMPs), rather than to HSCs (22). Furthermore, the gene expression profiles AML stem cells is similar to that of committed myeloid progenitors, suggesting that AML stem cells may be derived from myeloid progenitors. In addition, it has been reported that the expression pattern of genes that are associated with stem cell phenotypes in AML is similar to that in HSCs or embryonic stem cells (18, 22, 23). These find-

Conflict of interest: The authors have declared that no conflict of interest exists.
Citation for this article: *J Clin Invest.* 2012;122(6):2114–2129. doi:10.1172/JCI62279.

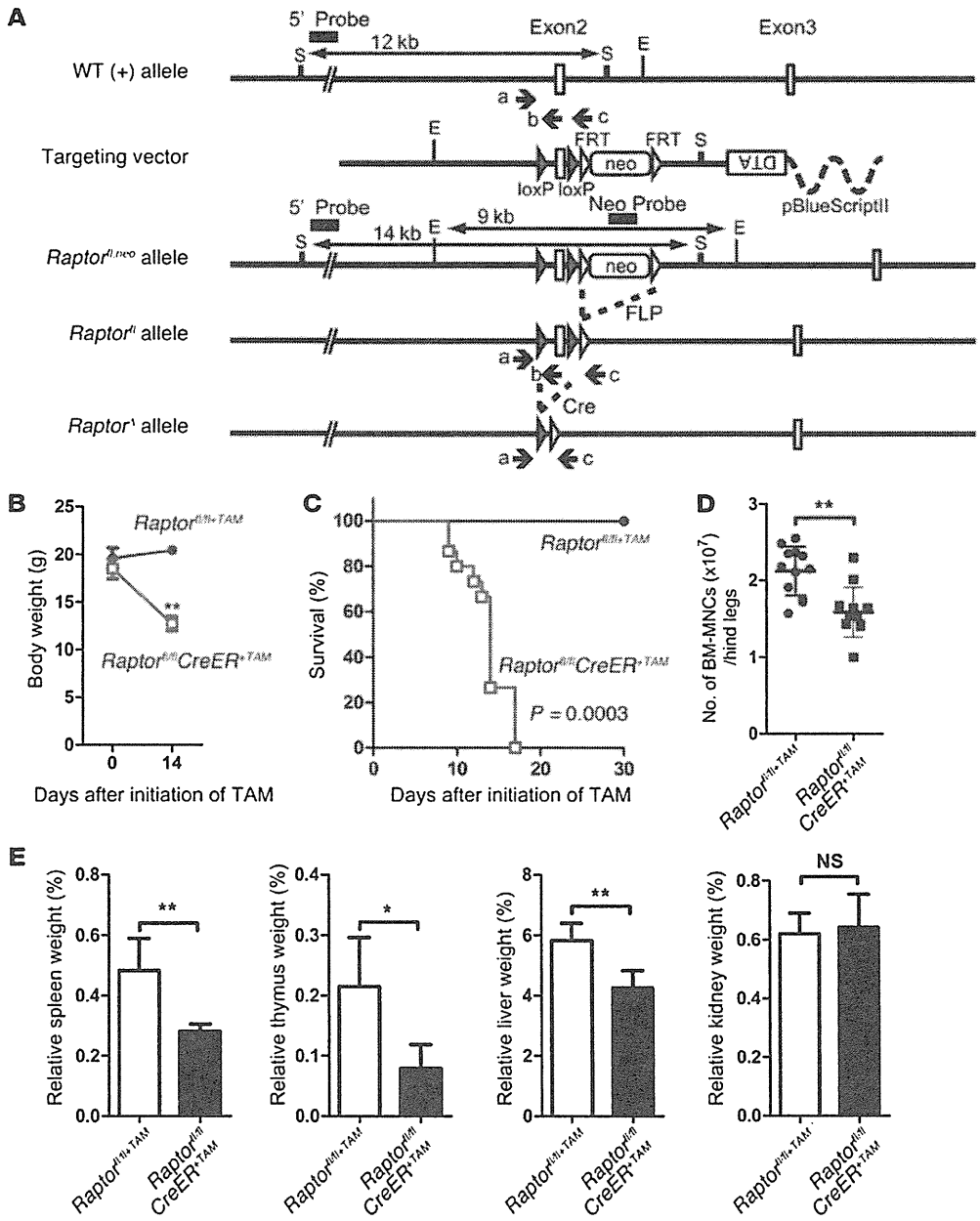

Figure 1

Conditional deletion of *Raptor* causes abnormalities in the hematopoietic organs of adult mice. (**A**) Targeting strategy to create the floxed *Raptor* (*Raptor*^{fl}) allele. The targeting vector includes a FRT-flanked neo cassette (PGK promoter–driven neomycin resistance gene) for positive selection and a diphtheria toxin A (DTA) gene for negative selection. *Raptor* exon 2 is flanked by loxP sites. The neo cassette of the *Raptor*$^{fl;neo}$ allele was removed by crossing *Raptor*$^{fl;neo}$ mice with *CAG-FLP* mice. Exon 2 was removed by Cre recombinase to give the *Raptor*$^{\Delta}$ allele. Probes for Southern blotting (5′ probe, Neo) and primers for PCR (a, b, c) are indicated. E, *Eco*RI; S, *Sac*I. (**B**) Body weight of *Raptor*$^{fl/fl+TAM}$ (control) and *Raptor*$^{fl/fl}$*CreER*$^{+TAM}$ (*Raptor*-deficient) mice. Data shown are the mean body weight ± SD (n = 5). (**C**) Survival of control and *Raptor*-deficient mice. P = 0.0003 (log-rank test; n = 15). (**D**) Decreased numbers of BM-MNCs. Data shown are the mean BM-MNC number ± SD in hind legs of control and *Raptor*-deficient mice at 10 days post-TAM (n = 12). (**E**) Organ weights of control and *Raptor*-deficient mice at 10 days post-TAM. Data shown are the mean relative organ weight (% of total body weight) ± SD (n = 5). $^{*}P < 0.05$, $^{**}P < 0.01$ (Student's t test).

ings suggest that AML stem cells originate from myeloid progenitors that have acquired stemness properties during leukemogenesis. Thus, determining how mTORC1 functions in both hematopoiesis and leukemia could provide novel insights into the mechanisms controlling the properties of CSCs.

Rapamycin and its derivatives are allosteric inhibitors of mTORC1 and likely inhibit its function through direct interaction. However, 4E-BP1, a direct target of mTORC1, is reportedly a rapamycin-insensitive substrate (24, 25). Two recent phosphoproteomic analyses revealed that there are critical differences between

rapamycin and ATP-competitive mTOR inhibitors (26, 27). Thus, genetic approaches will be likely be the most effective for inactivation of mTORC1 in vivo, because the regulation of mTORC1 by chemical inhibitors is complicated and may not produce predictable reductions in mTORC1 activity.

In this study, we generated mice with an inducible conditional deletion of *Raptor*, which encodes an essential component of mTORC1, and investigated the physiological and pathological roles of mTORC1 in normal and malignant hematopoiesis. These studies show striking evidence that the self-renewal and tumor-initiating properties of leukemia stem cells are differentially dependent on mTORC1.

Results

Conditional deletion of Raptor causes abnormalities in hematopoietic organs of adult mice. To investigate mTORC1 function in normal hematopoiesis in vivo, we used a tamoxifen-inducible (TAM-inducible) CreER system to generate mutant mice in which *Raptor* could be depleted in all tissues by i.p. injection of TAM (Figure 1A and Supplemental Figure 1, A and B; supplemental material available online with this article; doi:10.1172/JCI62279DS1). These *Raptor*$^{fl/fl}$*;Rosa-CreER*^{T2} mice are referred to herein as *Raptor*$^{fl/fl}$*CreER* mice before TAM administration and as *Raptor*$^{fl/fl}$*CreER*$^{+TAM}$ mice after TAM administration and *Raptor* deletion. The corresponding control mice, in which *Raptor* is not deleted, are referred to as *Raptor*$^{fl/fl+TAM}$ or *Raptor*$^{fl/+}$*CreER*$^{+TAM}$ mice. As expected, embryonic fibroblasts derived from *Raptor*$^{fl/fl}$*CreER*, but not from *Raptor*$^{fl/+}$*CreER*, mice showed loss of Raptor protein, resulting in dramatic inhibition of proliferation after TAM treatment (Supplemental Figure 1C). We also detected a remarkable reduction in p-S6 and p–4E-BP1 with Western blotting and by flow cytometry (Supplemental Figure 1, D and E), confirming that we had successfully established a system for the conditional inactivation of mTORC1. After administration of TAM, *Raptor*$^{fl/fl}$*CreER*$^{+TAM}$ mice rapidly lost body weight and died within 17 days, likely due to severe intestinal dysfunction, because we found dramatic loss of villi associated with increased apoptosis in the epithelial layer (Figure 1, B and C, and Supplemental Figure 1, F–I). At 10 days after the last TAM treatment (post-TAM), we found that the number of wbc in peripheral blood (PB), as well as mononuclear cells (MNCs) in BM, was significantly decreased in the absence of *Raptor* (Figure 1D and Supplemental Figure 2A). The masses of the thymus, spleen, and liver were also reduced in *Raptor*$^{fl/fl}$*CreER*$^{+TAM}$ mice compared with *Raptor*$^{fl/fl+TAM}$ mice (Figure 1E). These abnormalities were not observed in *Raptor*$^{fl/+}$*CreER*$^{+TAM}$ mice (Supplemental Figure 3, A and B), confirming that the phenotypes are caused by *Raptor* deletion and not by nonspecific effects of Cre expression.

Deletion of Raptor impairs granulocyte and B cell development but does not alter progenitor cell survival or proliferation. To examine which cell populations are affected by *Raptor* deletion, we analyzed BM-MNCs by flow cytometry with Abs to several cell surface markers. In particular, *Raptor* deficiency resulted in decreased numbers of Mac-1$^+$Gr-1$^+$ granulocytes, although the number of Mac-1$^+$Gr-1$^-$ myeloid lineage cells increased in BM (Figure 2A and Supplemental Figure 2, B, G, and H). *Raptor* deficiency led to dramatic decreases in B220^{lo}IgM$^-$ cells (early B cell precursors: pro/pre-B cells) and B220^{lo}IgM$^+$ cells (immature B cells), but not B220^{hi}IgM$^+$ cells (mature B cells) (Figure 2A and Supplemental Figure 2, I and J). These abnormalities were not observed in *Raptor*$^{fl/+}$*CreER*$^{+TAM}$ mice (Supplemental Figure 3C). In contrast to its effects on differentiated cells, *Raptor* deficiency was much less detrimental to hematopoietic progenitor cells. In the absence of *Raptor*, the number of common lymphoid progenitors (CLPs) was normal, and the number of GMPs was significantly increased (Figure 2A and Supplemental Figure 2, C–F). Importantly, the loss of differentiated cells in *Raptor*$^{fl/fl}$*CreER*$^{+TAM}$ mice appeared to be due to increased apoptosis in these populations (Lin$^+$ cells and Mac-1$^+$Gr-1$^+$cells), since *Raptor*-deficient c-Kit$^+$Sca-1$^-$Lin$^-$ (K$^+$S$^-$L$^-$) cells, including common myeloid progenitors (CMPs) and GMPs, did not show any obvious changes in apoptosis (Figure 2B). Cell cycle status as determined by in vivo BrdU incorporation was not altered by *Raptor* deficiency in any cell population examined (Figure 2C).

To evaluate the effect of *Raptor* deficiency on the colony-forming ability of myeloid cells in vitro, we isolated c-Kit$^+$Sca-1$^+$Lin$^-$ (K$^+$S$^+$L$^-$) cells, which include HSCs and multipotent progenitors (MPPs), or GMPs from the BM of *Raptor*$^{fl/fl}$*CreER*$^{+TAM}$ mice and cultured them in semisolid medium. Loss of Raptor dramatically inhibited formation of colonies with high proliferative potential in K$^+$S$^+$L$^-$ cells (Figure 2D and Supplemental Figure 4A). Retroviral transduction of human *RAPTOR* (*hRAPTOR*) rescued the defective colony-forming ability of *Raptor*-deficient K$^+$S$^+$L$^-$ cells (Supplemental Figure 4, B and C). In contrast, GMPs with and without *Raptor* showed comparable colony-forming abilities in this assay (Figure 2E and Supplemental Figure 4A). These data suggest that mTORC1 activity is not needed for the proliferation or differentiation of GMPs, but it may be essential for these processes in the more immature progenitor cells. To evaluate the activity of *Raptor*-deficient progenitor cells under more physiological conditions, we cultured K$^+$S$^+$L$^-$ cells on a layer of OP9 stromal cells. Whereas both B220$^+$ B cells and Mac-1$^+$ myeloid cells were generated from control K$^+$S$^+$L$^-$ cells under these culture conditions, *Raptor* deficiency strikingly decreased the number of B220$^+$ cells while increasing the number of Mac-1$^+$ cells (Figure 2F). In this culture condition, the emerging B cells are produced through *Raptor*-deficient B cell precursors; the defect in B cell precursors therefore resulted in decreased B cell production. Thus, these data are consistent with our in vivo observations (Figure 2A). To exclude the possibility that Raptor is needed for the microenvironment supporting hematopoiesis in vivo, we transplanted *Raptor*$^{fl/fl}$*CreER* BM-MNCs (CD45.2) plus the same number of competitor WT BM-MNCs (CD45.1/CD45.2) into recipient mice (CD45.1). At 2 weeks post-TAM, increased GMP and decreased granulocyte levels were present among *Raptor*$^{fl/fl}$*CreER*$^{+TAM}$ BM-MNCs (Supplemental Figure 5, A and B), also consistent with the flow cytometry data shown in Figure 2A. These findings indicate that the effects of *Raptor* deficiency on myeloid lineage cells are cell intrinsic and demonstrate that Raptor is not essential for the survival or proliferation of myeloid progenitor cells.

Raptor loss has differential effects on phosphorylation of mTORC1 effectors in different hematopoietic cell contexts. To investigate the effects of *Raptor* deficiency on mTORC1 signaling, we quantitatively evaluated the phosphorylation status of mTORC1 effectors by flow cytometric analysis using intracellular staining with an anti–p-S6 (S235/236) or anti–p-4E-BP1 (T36/45) Ab (Figure 3A), as we had done with embryonic fibroblasts (Supplemental Figure 1E). In control mice, the HSC/MPP (K$^+$S$^+$L$^-$) population contained both p-S6^{lo}p-4E-BP1^{lo} (HSC) and p-S6^{hi}p-4E-BP1^{hi} (MPP) cells. Control CMP and GMP populations mainly consisted of p-S6^{hi}p-4E-BP1^{hi} cells, whereas the majority of control B220$^+$ cells were p-S6$^{lo/neg}$p-4E-BP1$^{lo/neg}$, with a minority of p-S6^{hi}p-4E-BP1^{hi} cells. As expected, *Raptor* deficiency in vivo markedly decreased 4E-BP1 phosphory-

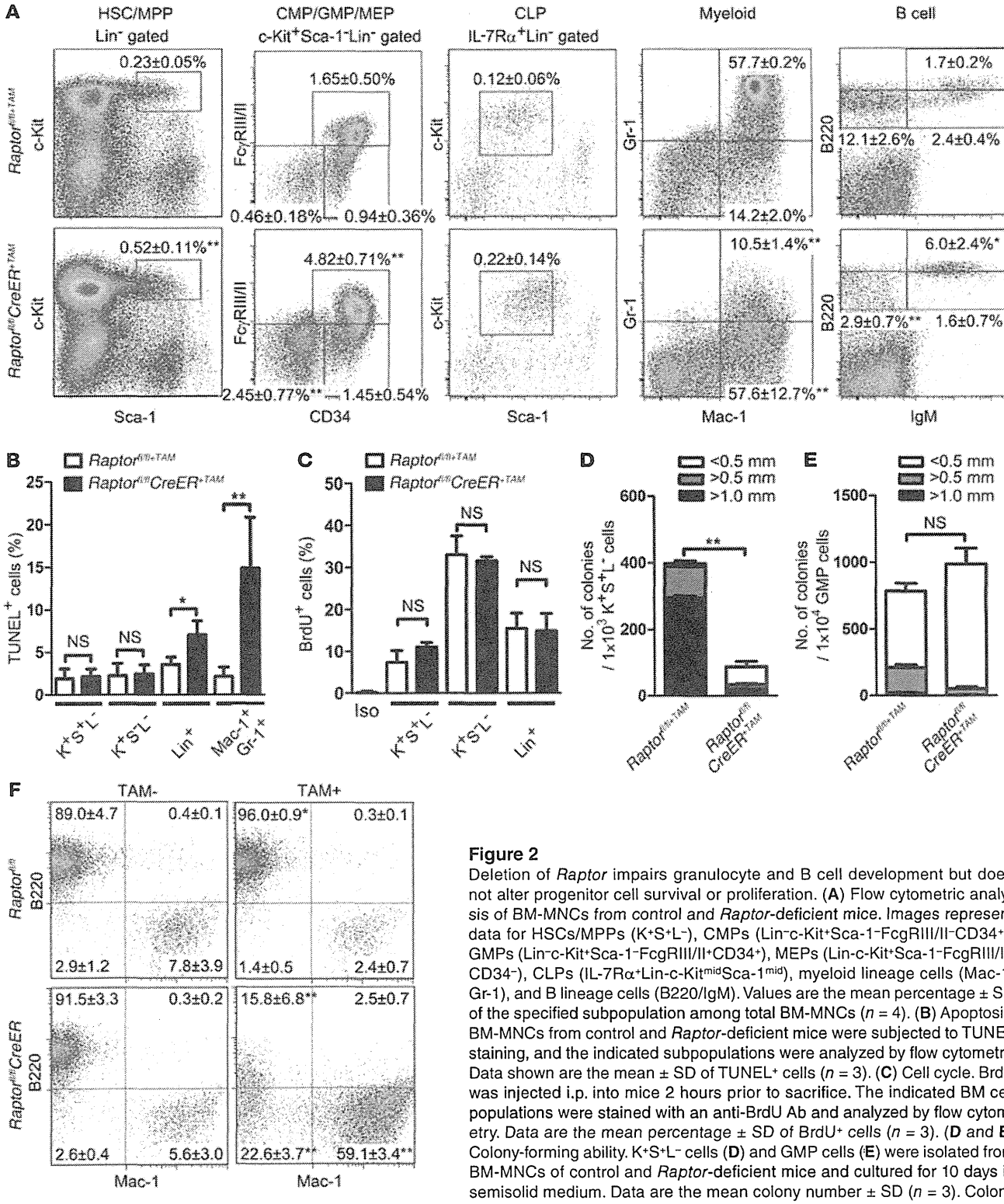

Figure 2

Deletion of *Raptor* impairs granulocyte and B cell development but does not alter progenitor cell survival or proliferation. (**A**) Flow cytometric analysis of BM-MNCs from control and *Raptor*-deficient mice. Images represent data for HSCs/MPPs ($K^+S^+L^-$), CMPs ($Lin^-c\text{-}Kit^+Sca\text{-}1^-FcgRIII/II^-CD34^+$), GMPs ($Lin^-c\text{-}Kit^+Sca\text{-}1^-FcgRIII/II^+CD34^+$), MEPs ($Lin\text{-}c\text{-}Kit^+Sca\text{-}1^-FcgRIII/II^-CD34^-$), CLPs ($IL\text{-}7R\alpha^+Lin\text{-}c\text{-}Kit^{mid}Sca\text{-}1^{mid}$), myeloid lineage cells (Mac-1/Gr-1), and B lineage cells (B220/IgM). Values are the mean percentage ± SD of the specified subpopulation among total BM-MNCs ($n = 4$). (**B**) Apoptosis. BM-MNCs from control and *Raptor*-deficient mice were subjected to TUNEL staining, and the indicated subpopulations were analyzed by flow cytometry. Data shown are the mean ± SD of $TUNEL^+$ cells ($n = 3$). (**C**) Cell cycle. BrdU was injected i.p. into mice 2 hours prior to sacrifice. The indicated BM cell populations were stained with an anti-BrdU Ab and analyzed by flow cytometry. Data are the mean percentage ± SD of $BrdU^+$ cells ($n = 3$). (**D** and **E**) Colony-forming ability. $K^+S^+L^-$ cells (**D**) and GMP cells (**E**) were isolated from BM-MNCs of control and *Raptor*-deficient mice and cultured for 10 days in semisolid medium. Data are the mean colony number ± SD ($n = 3$). Colony diameters are indicated. (**F**) Flow cytometric analysis of the differentiation into myeloid and B lineage cells of control and *Raptor*-deficient $K^+S^+L^-$ cells cultured on stromal cells. $Raptor^{fl/fl}$ or $Raptor^{fl/fl}CreER$ $K^+S^+L^-$ cells were cultured on a layer of OP-9 stromal cells for 2 weeks in the presence or absence of TAM. Data shown are the percentage ± SD of $B220^+$ $Mac\text{-}1^+$ cells among $CD45^+$-gated cells ($n = 3$). One flow cytometric analysis representative of 3 independent experiments is shown. $^*P < 0.05$, $^{**}P < 0.01$ (Student's *t* test).